



Energy Mines and
Resources Canada

Energie, Mines et
Ressources Canada

CANMET

Canada Centre
for Mineral
and Energy
Technology

Centre canadien
de la technologie
des minéraux
et de l'énergie

PERMEABILITY OF DIFFERENT MATERIALS TO RADON (^{222}Rn) GAS

J. BIGU, E.D. HALLMAN AND L. KENDRICK

ELLIOT LAKE LABORATORY

NOVEMBER 1991

Sudbury Neutrino Observatory Project Report SNO-STR-91-069.

MINING RESEARCH LABORATORY
DIVISION REPORT MRL 91- (TR)

PERMEABILITY OF DIFFERENT MATERIALS TO RADON (^{222}Rn) GAS

J. Bigu*, E.D. Hallman** and L. Kendrick***

ABSTRACT

The permeability of a variety of materials to ^{222}Rn has been measured in a Radon/Thoron Test Facility (RTTF) of the walk-in type. The measurements were conducted using an automated multi-sensor apparatus consisting of a number of ^{222}Rn passive monitors and meteorological sensors which permit simultaneous permeability studies of up to 12 different materials. Twenty-two different materials were tested. The permeability measured for these materials ranged from greater than about $1 \times 10^{-5} \text{ cm}^2\text{s}^{-1}$ to less than $-1.0 \times 10^{-9} \text{ cm}^2\text{s}^{-1}$. Among the several materials investigated, a number of them are suitable as ^{222}Rn barriers. However, for the special application intended here as wall-cover for restricting the flow of ^{222}Rn from mine walls (which require low permeability to ^{222}Rn , as well as great mechanical flexibility and resistance to impact) only two materials are potentially suitable, namely, an epoxy resin, and MIROCTM, a polyurethane-based material. Permeability studies are in progress to evaluate other materials for similar applications but different mechanical configurations.

Key words: Permeability; Radon; Diffusion.

*Research Scientist (MRL, CANMET, E.M.R.) and Adjunct Professor (Laurentian University); **Professor (Laurentian University); ***Research Technologist (Laurentian University).

CONTENTS

	<u>Page</u>
ABSTRACT	i
RESUME	ii
INTRODUCTION	1
THEORETICAL BACKGROUND	2
EXPERIMENTAL APPARATUS AND PROCEDURE	13
EXPERIMENTAL RESULTS AND DISCUSSION	15
EXPERIMENTAL DIFFICULTIES	20
CONCLUSIONS	22
ACKNOWLEDGEMENT	22
REFERENCES	23

TABLES

<u>No.</u>		
1.	Permeability of several materials to ^{222}Rn	25
2.	Diffusion length of ^{222}Rn in several materials	26

FIGURES

1.	Membrane geometry	25
2.	Normalized count rate versus elapsed time	26
3.	Radon-222 monitors showing geometrical arrangement used to determine the permeability of membranes	27
4.	'Multisensor' apparatus used to determine the permeability of membranes	28
5.	Alpha-particle count rate versus elapsed time for a glass fibre filter (upper trace) and a low permeability membrane (epoxy)	29

INTRODUCTION

A desirable feature of certain materials is their ability to separate the components of a gas mixture by diffusion processes. While some materials are quite effective in separating individual gases from a gas mixture diffusing through them, other materials are equally efficient in separating the components of a liquid mixture. In all these cases, the process of separation is related to the different rates at which different gases or liquids diffuse through the material. Materials that have the property of separating individual components from a gas or a liquid mixture are commonly referred to as membranes.

A variety of natural and artificial materials commonly available in the market have properties that make them ideally suitable for a variety of applications for industrial, chemical, medical, biological, pharmaceutical, commercial and research purposes (1-4). Practical applications of membranes are far too numerous to be listed here. Suffice to say that were it not for the properties of some biomacromolecules, that play a fundamental role in the diffusion of ions through living cells, biological systems would cease to exist. Some membrane materials are also useful in filtration and reverse osmosis processes.

In addition to a number of natural chemical compounds, a wide range of artificially produced materials, such as polymers, are potentially useful in a variety of separation applications. Included in this group of materials are silicone and hydrocarbon rubbers, polyethylenes, polypropylenes, polystyrenes, polysulfones, polycarbonates, polyesters, polyamides, and epoxies, to name but a few materials. The usefulness of some of these complex organic compounds is not restricted to their partial or total permeability to a given gas or liquid, i.e., fluid, or their different permeability to different fluids. Equally important in many applications is their very low, or even total lack of permeability to a particular type of

fluid. Materials with very low permeability characteristics to some particular fluid or group of fluids are usually referred to as 'barriers'. Clearly, the basic difference between a 'membrane' and a 'barrier' resides in their degree of permeability to a given fluid or group of fluids. Both types of materials are equally important in the context of this report.

In this report, the permeability characteristics of a number of common and rather specialized materials to radon (^{222}Rn) are investigated. Permeability data are of interest in the design of effective ^{222}Rn emissions from, say, underground mine cavities. Because ^{222}Rn is a naturally occurring radioactive gas whose γ -ray emitting progeny can interfere with the detection of neutrinos, the present study is of interest to the Sudbury Neutrino Observatory (SNO) which is to be built and operated in the Creighton Mine (Inco Ltd.), Ontario.

THEORETICAL BACKGROUND

The diffusion of gases through solids is governed by the first and second Fick's Law of Diffusion. The penetration of gases into and through solids, such as polymer membranes and other materials, by pure diffusive phenomena represents an idealized case. In actual practice, transport phenomena caused by pressure and temperature differentials between opposite sides of the material, as well as airflow, can significantly affect the penetration and penetration rate of gases into the solid.

In this work, processes other than diffusion will be ignored although frequent reference to experimental difficulties and practical aspects of the work will be made. But even in this simplified scheme, pure diffusive phenomena can be very complex. With regard to the gas/membrane system there are a number of cases of great practical interest:

1. The gas is chemically inert, and is, in addition, a stable isotope, i.e., it neither reacts chemically with the membrane or decays by radioactive

processes;

2. The gas is chemically active (it reacts chemically with the membrane) but, is a stable isotope;
3. The gas is chemically inactive with regards to the membrane, but is not a stable isotope;
4. The gas reacts chemically with the membrane, and, in addition, is not a stable isotope.

In the above cases it has been tacitly assumed that the membrane contains no radioactive isotopes, in other words, it is not a radioactive source itself. However, this is frequently not the case, e.g., most materials contain measurable amounts of ^{226}Ra which in turn decays into ^{222}Rn , the radioactive gas we are mainly interested in here.

The diffusion of a gas through a thin solid material such as a membrane can be described by the following expressions:

$$J = -SD(\partial C/\partial z)_{z=0} \quad (1)$$

$$\partial C/\partial t = D(\partial^2 C/\partial z^2) - KC + \phi \quad (2)$$

$$q(t) = \int_0^t J(t)dt \quad (3)$$

Equations 1 and 2 are the first and second Fick's Laws of diffusion, respectively. The meaning of the symbols used are as follows:

J is the flux density of gas through the material (membrane),

D is the diffusion coefficient of the gas in the material,

S is the surface area of the material,

C is the concentration of gas in the material,

z is the coordinate, i.e., distance from an arbitrary origin,

ϕ is the radioactive source term of the material, i.e., the rate of production of radioactive gas in the membrane,

K is the quantity that characterizes chemical reactions taking place between the gas and the membrane, as well as the radioactive decay of the gas, λ , diffusing through the membrane,

$q(t)$ is the quantity of gas passing through the membrane.

In the more general case, the quantity K can be written:

$$K = k_R + \lambda \quad (4)$$

where, k_R is the reaction constant for the first-order chemical process, and λ is the radioactive decay constant of the gas diffusing through the membrane.

In the case investigated in this work, a number of simplifications can be introduced:

- A. Because of the relatively high chemical inertness of ^{222}Rn and ^{220}Rn (5), one can safely assume for our particular case: $k_R = 0$. Hence, $K = \lambda$;
- B. In general, the ^{226}Ra content in the membrane materials is quite low, and hence, it mainly results in the production of some additional ^{222}Rn which will diffuse through the membrane resulting in small contributions to the total ^{222}Rn concentration measured at the opposite side of the membrane (see experimental procedure). The same reasoning applies to ^{224}Ra in the membrane and its decay into ^{220}Rn . However, the problem becomes more complex if the diffusion of a radioactive gas is measured in a membrane containing a radioisotope which upon decay produces a radioactive gas different from the one being measured, e.g., ^{224}Ra when measuring ^{222}Rn , or ^{226}Ra when measuring ^{220}Rn . As we shall see, the conditions of the experiment can be set to reduce the contribution(s) discussed here to a negligible amount. Under these conditions, one can safely set: $\phi = 0$. (Note: it is assumed that the radioactive source does not induce material damage thereby changing the characteristics of the membrane.)

Taking the above discussion into account, i.e., items A and B, our case reduces to solving the situation depicted in item 3, and Equation 2. reduces to:

$$\partial C / \partial t = D(\partial^2 C / \partial z^2) - \lambda C \quad (5)$$

Expressions 1, 3 and 5 can be solved using the standard methods of mathematical physics (6,7) and Figure 1 (which shows the geometry

of the problem), taking into account the boundary conditions:

$$C(0,t) = 0, \quad C(\delta,t) = C_0, \quad C(z,0) = 0 \quad (6)$$

where, δ is the thickness of the membrane. The symbol C_0 is used to denote the concentration of ^{222}Rn (or ^{220}Rn) 'outside' the membrane. This concentration is assumed to remain constant during the measurements and experiment (see Figure 1 and Experimental Procedure).

With the above in mind, it can be shown that the concentration distribution across the membrane of thickness δ with time t , i.e., $C(z,t)$, is given by (8):

$$C(z,t) = \frac{C_0 z}{\delta} + \frac{2C_0 \lambda}{\pi} \sum_{n=1}^{\infty} \frac{(-1)^n \sin(n\pi z/\delta)}{n(n^2 B + \lambda)} [1 - e^{-(n^2 B + \lambda)t}] \\ + \frac{2C_0}{\pi} \sum_{n=1}^{\infty} \frac{(-1)^n}{n} \sin(n\pi z/\delta) e^{-(n^2 B + \lambda)t} \quad (7)$$

where, in Equation 7 the quantity B is given by:

$$B = \pi^2 D / \delta^2$$

The flux density, J , i.e., number of atoms (^{222}Rn or ^{220}Rn) crossing the membrane of surface area A at a point $z=0$ (see Figure 1) per unit time can be calculated by substituting Equation 7 into Equation 1:

$$J(t) = -DA(\partial C/\partial z)_{z=0} \\ = \frac{DA C_0}{\delta} \left[1 + 2 \sum_{n=1}^{\infty} (-1)^n e^{-(n^2 B + \lambda)t} \right. \\ \left. + 2\lambda \sum_{n=1}^{\infty} \frac{(-1)^n}{n^2 B + \lambda} (1 - e^{-(n^2 B + \lambda)t}) \right] \quad (8)$$

The total number of atoms crossing the membrane in time t , i.e., $q(t)$, can be calculated substituting Equation 8 into Equation 3. After some algebraic manipulations the result is:

$$\begin{aligned}
q(t) &= \int_0^t J(t) dt = -A \int_0^t D(\partial C/\partial z)_{z=0} dt \\
&= \frac{DA C_0}{\delta} \left[t + 2 \sum_{n=1}^{\infty} \frac{(-1)^n}{n^{2B+\lambda}} (1 - e^{-(n^{2B+\lambda})t}) \right. \\
&\quad + 2\lambda t \sum_{n=1}^{\infty} \frac{(-1)^n}{n^{2B+\lambda}} \\
&\quad \left. - 2\lambda \sum_{n=1}^{\infty} \frac{(-1)^n}{(n^{2B+\lambda})^2} (1 - e^{-(n^{2B+\lambda})t}) \right] \quad (9)
\end{aligned}$$

Under steady-state conditions, i.e., conditions at $t \rightarrow \infty$, Equation 8 becomes:

$$J(t \rightarrow \infty) = J_{\infty} = \frac{DA C_0}{\delta} \left[1 + 2\lambda \sum_{n=1}^{\infty} \frac{(-1)^n}{n^{2B+\lambda}} \right] \quad (10)$$

Equation 9 on the other hand indicates that $q(t)$ is composed of a linear part and an exponential contribution. For sufficiently large values of t , i.e., $t \rightarrow \infty$ the exponential term becomes very small, i.e.,

$$1 \gg e^{-(n^{2B+\lambda})t}$$

and Equation 9 reduces to:

$$q(t \rightarrow \infty) = q_{\infty} = \frac{DA C_0}{\delta} \left[t + 2 \sum_{n=1}^{\infty} \frac{(-1)^n}{n^{2B+\lambda}} + 2\lambda t \sum_{n=1}^{\infty} \frac{(-1)^n}{n^{2B+\lambda}} - 2\lambda t \sum_{n=1}^{\infty} \frac{(-1)^n}{(n^{2B+\lambda})^2} \right] \quad (11)$$

Equation 11 shows the linear growth of $q(t)$. For a time $t = \theta$ at which $q(t) = 0$, Equation 11 becomes:

$$\theta \left[1 + 2\lambda \sum_{n=1}^{\infty} \frac{(-1)^n}{n^{2B+\lambda}} \right] = 2\lambda \sum_{n=1}^{\infty} \frac{(-1)^n}{(n^{2B+\lambda})^2} - 2 \sum_{n=1}^{\infty} \frac{(-1)^n}{n^{2B+\lambda}} \quad (12)$$

But it can easily be shown that the right hand side (rhs) of Equation 12 is:

$$\text{rhs} = 2 \sum_{n=1}^{\infty} \frac{(-1)^n n^{2B}}{(n^{2B+\lambda})^2} \quad (13)$$

From Equations 12 and 13 the time θ at which $q(t) = 0$, i.e.,

intercepts the time axis, can be calculated:

$$\theta = \frac{2 \sum_{n=1}^{\infty} \frac{(-1)^n n^2 B}{(n^2 B + \lambda)^2}}{1 + 2\lambda \sum_{n=1}^{\infty} \frac{(-1)^n}{n^2 B + \lambda}} \quad (14)$$

The quantity θ , is called the time-lag and can be calculated from experiment (see Figure 2). Since $B = \pi^2 D / \delta^2$, and λ and δ are known or can be measured, Equation 14 can be used to calculate D during the early phase of the diffusion process, i.e., linear growth as opposed to measurement at steady-state conditions, i.e., $t \rightarrow \infty$.

It is easy to show that Equation 14 reduces to the well known (simple) time-lag expression for a stable diffusing gas (3,9). For the case of $\lambda=0$ (stable gas), Equation 14 becomes:

$$\theta(\lambda=0) = (2\delta^2 / \pi^2 D) \sum_{n=1}^{\infty} (-1)^n / n^2 \quad (15)$$

The summation term $\sum_{n=1}^{\infty} (-1)^n / n^2$ can be calculated using the

summation of series general expression:

$$\begin{aligned} & (1/1^{2p}) - (1/2^{2p}) + (1/3^{2p}) - (1/4^{2p}) + \dots \\ & = \frac{(2^{p-1} - 1) \pi^{2p} B_p}{(2p)!} \end{aligned} \quad (16)$$

where, B_p is the Bernoulli's number of index p . Equation 16 applies to Equation 15 for $p=1$ for which $B_p = B_1 = 1/6$. Hence:

$$\sum_{n=1}^{\infty} (-1)^n / n^2 = \pi^2 / 12 \quad \text{and,}$$

$$\theta(\lambda=0) = \delta^2 / 6D \quad (17)$$

Equation 17 is identical to the expression given for the stable isotope case given by several authors (3,9).

As previously indicated, Equation 14 can be used to calculate D from graphical analysis of the data. Likewise, Equation 10 can be used to determine D although the procedure is somewhat more involved.

The theory presented above is readily applicable to the case for which the following boundary condition is satisfied: $C(x=0) = 0$ at $t > 0$ (see Equation 6 and the geometry of the arrangement shown in Figure 1). This is the case for which the flow of radioactive gas through the membrane occurs under the maximum concentration gradient ($\delta C / \delta z = (C_0 - 0) / (\delta - 0)$) possible. In other words, when the concentration of radioactive gas in the receiver volume, V_2 (the volume downstream of the membrane where the radioactive gas is 'collected') is negligible compared with C_0 , the concentration upstream of the membrane. This condition is met when V_2 is large, or when the diffusion coefficient, D, of the radioactive gas in the membrane material is very small, or both.

When the condition $C(x=0) > 0$ at $t > 0$ is met rather than the condition previously indicated above, the theory describing the diffusion process requires some modification and a different theoretical approach has been developed and applied (10). This condition applies to the case of membranes with moderate and high diffusion coefficients through which the radioactive gas diffuses into a well-stirred small receiver volume, V_2 . Under these experimental conditions, $C(x=0)$ at $t > 0$ represents the actual concentration of radioactive gas in V_2 , namely, $C(V_2) = C(x=0)$ at $t > 0$.

In the remainder of this section, a different theoretical approach to the diffusion of a radioactive gas through membranes is presented. This theory, although somewhat less rigorous than the one discussed above and the one described elsewhere (10) is simpler experimentally and analytically. The theoretical approach described here has been discussed elsewhere (11), and

has been used at our Laboratory in conjunction with a multisensor apparatus which was designed and developed for comparative membrane ^{222}Rn and ^{220}Rn permeability studies (12).

With the geometry sketched in Figure 3 with a source of N_1 atoms of ^{222}Rn or ^{220}Rn in volume V_1 , i.e., the radioactive gas reservoir, separated from the sensitive volume, V_2 , of a ^{222}Rn (^{220}Rn) gas monitor by a membrane of thickness δ , surface area A , and permeability k , one may write the kinetic equations describing the gas diffusion process as follows:

$$dN_1/dt = -\lambda N_1 + \phi - QN_1/V_1 - (kA/\delta V_1) (N_1 - N_2) \quad (18)$$

and,

$$dN_2/dt = -\lambda N_2 + (kA/\delta V_2) (N_1 - N_2) \quad (19)$$

where,

N_2 is the number of atoms of ^{222}Rn or ^{220}Rn in volume V_2 ,

ϕ is the production rate of ^{222}Rn or ^{220}Rn in volume V_1 ,

Q is the airflow rate in volume V_1 ,

λ is the radioactive decay constant of ^{222}Rn or ^{220}Rn .

k = permeability

The first, third, and fourth terms on the right hand side of Equation 18 describe, respectively, the removal of the radioactive gas in volume V_1 by radioactive decay, mechanical (forced) ventilation, or airflow, and diffusion through the membrane. The first and second terms on the right hand side of Equation 19 describe, respectively, the removal of radioactive gas in V_2 by radioactive decay, and the increase in gas concentration in the same volume by diffusion of gas from V_1 through the membrane.

Equations 18 and 19 can be rearranged as follows:

$$(dN_1/dt) + MN_1 = \phi + SN_2, \text{ and} \quad (20)$$

$$(dN_2/dt) + PN_2 = TN_1 \quad (21)$$

where,

$$M = \lambda + (kA/\delta V_1), \quad \Lambda = \lambda + (Q/V_1) \quad (22)$$

$$S = kA/\delta V_1, \quad P = \lambda + (kA/\delta V_2), \quad T = kA/\delta V_2 \quad (23)$$

However, as soon as the radioactive gas starts diffusing from V_1 into the sensitive volume, V_2 , of the membrane and detector arrangement, it immediately starts decaying into its short-lived decay products (progeny). The rate of growth of these radioactive products can be expressed as follows:

$$dN_i/dt = N_{i-1} \lambda_{i-1} - N_i \lambda_i \quad (24)$$

where the index i in the above expression refers to ^{218}Po , ^{214}Po and ^{214}Bi (^{214}Po) for the ^{222}Rn progeny, and ^{216}Po , ^{212}Pb , ^{212}Bi and ^{212}Po for the ^{220}Rn progeny. The index $i-1$ refers to the parent products of the decay product i , i.e., ^{222}Rn for ^{218}Po , and so on.

The solution to Equation 21 can be simplified as in our case $dN_i/dt = 0$ for the ^{222}Rn concentration in V_1 . (The reader should be aware that experiments have been conducted in a large radioactivity-controlled Radon/Thoron Test Facility (RTTF) of the walk-in type. Hence, steady-state conditions are easily attained.)

After some algebraic manipulation, and taking into account the boundary conditions:

$$N_1(t=0) = N_1, \quad N_2(t=0) = 0$$

it is easy to show that:

$$N_2 = (E/K) (1 - e^{-Kt}) \quad (25)$$

where,

$$E = \phi T/M \quad \text{and} \quad K = P - (ST/M) \quad (26)$$

Correspondingly more complex expressions are obtained from Equation 24 for N_i , as shown elsewhere (13,14). It can be shown that the activities $N_2 \lambda$ and $N_i \lambda_i$ in V_2 reduce to a constant value $\lambda(E/K)$ for large values of t (13,14). The ratio E/K is given, after some algebraic manipulation, by:

$$E/K = \frac{\phi}{\Lambda} \frac{1}{1 + \left(\frac{\lambda \delta}{k}\right) \left(\frac{V_2}{A}\right)} \quad (27)$$

If an α -particle detector of geometrical α -counting efficiency ϵ in a given volume, i.e., V_2 , is used, the α -count rate recorded by the detector, N_α , is given by:

$$N_\alpha = \epsilon(N_2\lambda + \sum_i N_i\lambda_i) = \Omega(E/K) \quad (28)$$

where the symbol Ω represents a proportionality factor which depends on ϵ and other variables.

Equations 27 and 28 can be used to determine the permeability k . This is most readily done by comparing data, i.e., α -particle count, obtained with two ^{222}Rn gas monitors, one covered with the membrane of interest and the other covered with a porous material of sufficiently high permeability to allow free passage of the radioactive gas while still removing its decay products. Under steady-state conditions, i.e., for $Kt \gg 1$ it is easy to show from Equations 27 and 28 that:

$$N_{\alpha m}/N_{\alpha p} = R_{m,p} = \frac{1}{1 + \left(\frac{\lambda\delta}{k}\right) \left(\frac{V_2}{A}\right)} \quad (29)$$

Hence, from Equation 29, one obtains k :

$$k = \left(\frac{\delta V_2}{A}\right) \lambda \varphi \quad (30)$$

$$\text{where, } \varphi = R_{m,p}/(1 - R_{m,p}) \quad (31)$$

The approach discussed above has the advantage that only measurements under steady-state conditions, i.e., $t \rightarrow \infty$ for which $dN_2/dt = 0$, need to be accurate. This considerably simplifies the experimental procedure and reduces man-power requirements. However, it also has some drawbacks, namely:

1. The exposure time necessary to attain steady-state conditions in V_2 may take several days depending on k . This requires a highly stable reservoir of ^{222}Rn or ^{220}Rn ;
2. Equations 18 and 19 are only approximate because the terms $kA(N_1 - N_2)/\delta V_1$ and $kA(N_1 - N_2)/\delta V_2$ assume that a steady-state is instantaneously

established across the membrane for a given concentration gradient. This assumption is only satisfied if the diffusion length $DL = (D/\lambda)^{1/2}$ and the time-lag $\theta = \delta^2/6D$ ~~which~~ satisfy the following requirements:

$$DL \gg \delta \quad \text{and} \quad \theta \ll 0.693/\lambda \quad (32)$$

For ^{222}Rn , the inequality $\theta \ll 0.693/\lambda$ can be rewritten as $\theta \ll 3.82 \text{ d}$. This condition is fairly easy to verify from experimental values of θ obtained by graphical analysis of the data. If the condition $\theta \ll 3.82 \text{ d}$ is met, Equation 17 (which applies for the stable isotope case, i.e., $\lambda=0$) can be used to calculate D . With this tentative value of D , the diffusion length $DL = (D/\lambda)^{1/2}$ can be calculated and the condition $DL \gg \delta$ can be checked. (One way of meeting the requirement $DL \gg \delta$ is by reducing (choosing) the thickness of the membrane under consideration, accordingly. However, this is not always possible or practical.) If both conditions indicated by Equation 32 are met, the simplified version for the time-lag can be used to calculate D instead of the much more complex expression given by Equation 14.

It should be noted that the diffusion 'constant' D , and the permeability, k , of a membrane are related by the simple expression:

$$k = sD \quad (33)$$

where, s is the solubility of the membrane.

The solubility of the membrane can be written as:

$$s = c(f)\eta \quad (34)$$

where, $c(f)$ is a conversion factor, and η is a dimensionless ratio which stands for the concentration of gas inside the pores of the solid (membrane) to the concentration of gas outside the solid. If the pressure of the gas outside the material is the same as the pressure inside, the quantity η is the same as the porosity of the medium, provided that the gas inside the pores in the solid behave like an ideal gas.

EXPERIMENTAL APPARATUS AND PROCEDURE

The diffusion characteristics of ^{222}Rn through membranes was studied by means of ^{222}Rn monitors of the passive kind using a solid-state detector of the diffused-junction (DJ) type in conjunction with its associated preamplifier/amplifier system and other electronic circuitry. The detector and associated electronic circuitry are located in a stainless steel cylindrically-shaped case (34 cm long, 5 cm outer diameter). The DJ detector is located about 8 cm from the open end of the stainless steel case, thereby providing a well defined volume, i.e., V_2 (see Equations 18 and 19). The DJ detector is protected by an aluminized mylar sheet covering the detector. A (removable) plastic grid located at about 2 cm from the open end of the case protects the detector against accidental damage.

Because meteorological variables play an important role in gas diffusion and transport processes, sensors to monitor barometric pressure (P), temperature (T), air velocity (v) and direction, and relative humidity (RH), were also used in conjunction with the ^{222}Rn monitors. The ^{222}Rn monitors and the meteorological sensors were interfaced to a data logger with programmable sampling time from 1 min to 999 min in steps of 1 min. Digital output sensors (^{222}Rn monitors) could be programmed independently of analog sensors (meteorological sensors). A total of 12 ^{222}Rn monitors and 8 analog sensors could be logged into the data logger. Data were printed in 'real-time' and stored in a personal computer (PC) for further graphical and statistical analysis.

Samples of the membranes of interest were cut in a circular shape and sandwiched tightly between two circular flanges. One flange was attached to the end of the steel case housing the DJ detector and its associated electronic circuitry. The other flange was free. The two flanges were brought together by means of threaded screws, nuts and washers thus providing a leak free seal when the membrane was in place.

All the ^{222}Rn monitors were used simultaneously with different types of membranes except for one monitor which was used with glass fibre (GF) filter material as the reference ^{222}Rn monitor. The GF material was used to remove ^{222}Rn progeny while still allowing ^{222}Rn to diffuse through it easily.

The ^{222}Rn monitors, the meteorological sensors and the data logger are manufactured by Alpha-NUCLEAR (Toronto) and are known under the following commercial names: model 601 (^{222}Rn monitor); model 604 (P sensor); model 602 (air T probe); model DS 608 (dew point sensor); and model 650 (data logger). In this series of measurements a modified version of the experimental apparatus shown in Figure 4 was used (12).

Measurements were conducted in a large Radon/Thoron Test Facility (RTTF) of the walk-in type. The data logger and computer system were located outside the RTTF, whereas the ^{222}Rn monitor and meteorological sensors were placed inside it and connected to the data logger and computer system via signal cables running through one of the test facility walls. The sampling time was set at 1 h for most cases, depending on the type of membranes used, and the ^{222}Rn concentration. At a given time the ^{222}Rn monitors were introduced into the RTTF where they were connected to their corresponding signal cables, and measurements began. The increase in α -particle activity as determined by the ^{222}Rn monitors versus time was followed until steady-state conditions were attained. A careful record of meteorological data was kept.

Because of differences in DJ detector efficiency to α -particles and electronic circuitry characteristics, the ^{222}Rn monitors used in membrane permeability measurements were often calibrated in order to correct for differences in ^{222}Rn monitor sensitivity. Calibrations were carried out using glass fibre (GF) filter material as the 'membrane reference' material in the ^{222}Rn monitors, which were all exposed simultaneously to identical environmental conditions of ^{222}Rn concentration, T, P, and RH. The data were

used to calculate the calibration factor (CF) for each ^{222}Rn monitor in cph/pCiL^{-1} and cph/Bqm^{-3} , where cph stands for counts per hour.

After background (B) and sensitivity (CF) corrections were applied to the α -count rate obtained by each ^{222}Rn monitor, the data were used in the fashion indicated in Equation 30 in order to calculate k for each membrane.

The obvious advantage of using a multisensor apparatus, such as the one described here, is clear. First, it allows simultaneous determination of the permeability (k) and diffusion coefficient (D) of several membranes to the same radioactive gas, thereby minimizing the errors associated with the more conventional method whereby one membrane is measured at a time. Second, it relaxes certain restrictions regarding the constancy and degree of accuracy with which the radioactive gas concentration should be known, and maintained, during experimentation. Third, it provides a rapid means of comparing the characteristics of several materials with minimum effort.

EXPERIMENTAL RESULTS AND DISCUSSION

A summary of the experimental results obtained is given in Tables 1 and 2. Figure 2 shows a typical run where the normalized α -particle count rate has been plotted versus the time elapsed from the time the diffusibility experiment began. The data have been somewhat smoothed out for clarity of presentation. The y-axis (normalized count rate, dimensionless quantity) represents the ratio of the ^{222}Rn concentration [^{222}Rn], measured in the volume $V_2(m)$ (see Equations 18 and 19) enclosed by the membrane under investigation, to the [^{222}Rn] measured in $V_2(\text{GF})$ enclosed by the reference material, i.e., glass fibre filter (GF). In our case, $V_2(m) = V_2(\text{GF})$, where m stands for membrane. The square brackets are used to indicate concentration. The [^{222}Rn] is measured in each case by the DJ detector enclosed in V_2 in the

' α -meters', i.e., ^{222}Rn monitors calibrated prior to any diffusion experiment in a known ^{222}Rn concentration atmosphere, which is accurately measured by the Two Filter Tube (2FT) method (15,16), and by scintillation cells calibrated using a traceable ^{222}Rn standard source. Figure 2 is typical of these types of experiments, and is composed of three parts: a) a slow increase in [^{222}Rn] at the start until ^{222}Rn 'break-through' of the gas in the membrane is attained; b) a linear increase in [^{222}Rn]; c) a steady-state condition attained when the rate of ^{222}Rn diffusing through the membrane into V_2 equals the rate of decay of ^{222}Rn already in V_2 . Curves like Figure 2 are used to determine graphically the time-lag, θ (see Equations 14 and 17), from which the diffusion coefficient, D , can be calculated. This procedure and its result for a typical case will be illustrated below.

Figure 5 shows an example of a typical run in which the response of an epoxy membrane (lower trace) is compared with the response for the reference material (GF), upper trace. The α -particle count-rate fluctuations are partly due to the statistics of counting, and to the following factors:

1. Barometric pressure variations;
2. Airflow rate fluctuations in the Radon/Thoron Test Facility (RTTF) where the measurements are carried out (see the variable Q in Equation 18);
3. Air turbulence in the RTTF caused by mixing fans of the 'rotating' type whose operation is important for adequate ^{222}Rn air mixing, and hence, to produce a uniform and isotropic [^{222}Rn] throughout V_1 , i.e., the volume of the RTTF.

It should be noted that when V_2 is enclosed by the membrane, the air in V_2 is essentially 'trapped' at the ambient pressure prevailing at the time this operation takes place. Subsequent barometric pressure (P) variations induce pressure differentials, ΔP , between the two sides of the membrane, thereby causing in-flow or out-flow of ^{222}Rn through

the membrane material by convective transport mechanisms. The operation of the fan(s) also causes potentially strong disturbances on the outer side of the membrane, namely, positive pressure when the fan is pointing at the membrane and a negative pressure when it is pointing away from the membrane. This causes strong air currents and pressure differentials which encourage convective transport of ^{222}Rn through the membrane.

The contribution to the flow of ^{222}Rn through materials from convective transport mechanisms is rather complex and beyond the scope of this report, particularly when variable pressure perturbations are externally imposed on pure diffusion processes. The effects caused by the above perturbations depend a great deal on the diffusion coefficient and permeability of the material. The effect will be considerably accentuated if 'microscopic' pinholes, i.e., mechanical defects in the material are present.

It is not difficult to realize that the effect of items 1 to 3, combined with statistics of counting, can easily account for the α -particle count rate fluctuations observed during some of the experiments.

Table 1 presents permeability, k , data for a variety of materials. Also shown in the table are the values measured for the thickness of the different materials investigated. The data represent the result of nine independent experiments. Each experiment consisted of measuring the permeability of several materials at the same time. When possible, the materials are identified according to their commercial name. If the latter was not known, various means of identification were used according to what was known about the material. A quick glance at Table 1 suggests that the materials investigated fall into four groups or categories, namely:

1. Low permeability : $k < 1.0 \times 10^{-9} \text{ cm}^2 \text{ s}^{-1}$
2. Medium permeability : $1.0 \times 10^{-7} \text{ cm}^2 \text{ s}^{-1} > k > 1.0 \times 10^{-8} \text{ cm}^2 \text{ s}^{-1}$
3. High permeability : $k > 1.0 \times 10^{-6} \text{ cm}^2 \text{ s}^{-1}$
4. Very high permeability : i.e., 'transparent' to ^{222}Rn .

The values assigned to k , according to the permeability classification given above, are totally arbitrary and only meant to bring to the attention of the reader the broad range of experimental values found for k for the several materials (~20) investigated. In terms of performance, materials with $k \leq 1.0 \times 10^{-9} \text{ cm}^2 \text{ s}^{-1}$ can be considered good barriers to ^{222}Rn , i.e., diffusion of ^{222}Rn through these materials is totally impeded. The material with the lowest permeability measured was that of Kapton-Polyamide film, for which $k \sim 9.5 \times 10^{-10} \text{ cm}^2 \text{ s}^{-1}$. Materials with k in the range $1.0 \times 10^{-7} \text{ cm}^2 \text{ s}^{-1}$ to $1.0 \times 10^{-8} \text{ cm}^2 \text{ s}^{-1}$ are fairly good barriers, i.e., they only allow a small fraction of the ^{222}Rn to diffuse through. The best materials in this permeability range are listed (in no particular order) below:

1. Epoxy resins (manufactured by BMS Mfg. Inc., trade mark Oxyguard):
 $k \sim 3.5 \times 10^{-8} \text{ cm}^2 \text{ s}^{-1}$;
2. MIROC (a polyurethane-based material manufactured by URYLONTM):
 $k \sim 3.0 \times 10^{-8} \text{ cm}^2 \text{ s}^{-1}$;
3. Saranex (commercial name, manufactured by Dow Canada, material used for wrapping foods):
 $k \sim 3.7 \times 10^{-8} \text{ cm}^2 \text{ s}^{-1}$;
4. "Anti-thoron" membrane (obtained from Terradex, U.S.A., a commercial firm specializing in track etch nuclear measurements):
 $k \sim 7.9 \times 10^{-8} \text{ cm}^2 \text{ s}^{-1}$;
5. Coated polyester (obtained from 3M):
 $k \sim 5.3 \times 10^{-8} \text{ cm}^2 \text{ s}^{-1}$;
6. Saran wrap (commercial name, material used for wrapping foods; high density polyethelene):
 $k \sim 1.0 \times 10^{-8} \text{ cm}^2 \text{ s}^{-1}$;
7. Aluminized mylar:
 $k \sim 5.2 \times 10^{-8} \text{ cm}^2 \text{ s}^{-1}$;
8. Freezer bags (manufactured by Glad, commercial firm):

$$k \sim 7.8 \times 10^{-8} \text{ cm}^2 \text{ s}^{-1};$$

9. Mylar (manufactured by DuPont):

$$k \sim 1.6 \times 10^{-8} \text{ cm}^2 \text{ s}^{-1};$$

10. Aluminum foil (identified as Foil - Stuart House):

$$k \sim 4.6 \times 10^{-8} \text{ cm}^2 \text{ s}^{-1};$$

Materials of permeability significantly higher than $1.0 \times 10^{-6} \text{ cm}^2 \text{ s}^{-1}$ can be used in general as membranes through which ^{222}Rn can diffuse relatively easily while acting as a water vapour barrier. This is a very attractive feature with special application in instrumentation designed for assaying ^{222}Rn by passive methods.

Materials that allow ^{222}Rn to diffuse freely through them while removing its decay products are in the context of this research of particular use as 'reference' materials. Some of these materials include 'porous' polyurethanes, and filter materials such as cellulose acetates and nitrates and glass fibre (GF). The latter material (GF) has been used extensively here as the reference material in order to calculate k by the simplified method described in this work (see Equation 30). It should be noted, however, that the same experimental data obtained in this work can be used in conjunction with other theoretical approaches in order to obtain the diffusion coefficient, D . This will be shown in a forthcoming report.

It has been indicated above that in order for the simplified theoretical approach (Equations 18 to 31) to be applicable to a radioactive gas such as ^{222}Rn , the following two conditions must be met:

$$\theta = \delta^2/6D \ll 0.693/\lambda, \quad \text{and} \quad DL = (D/\lambda)^{1/2} \gg \delta \quad (32)$$

Time-lag (θ) analyses of the samples (see for example Figure 2 which will be discussed below) show that $\theta < 30$ h; whereas $0.693/\lambda = 3.82$ d ~ 92 h. Hence, the first condition (left hand side of Equation 32) is satisfied. The second condition (right hand side of Equation 32) can only be approximately tested because the diffusion coefficient, D , is not obtained

directly from the procedure used here. However, setting $D \approx k$, an approximate value for the diffusion length (DL) can be obtained (see Table 2). It can be seen that the condition $DL \ll \delta$ is amply satisfied for all the materials investigated here, except for the thicker samples of MIROC where this condition is marginally met. From the above, one may surmise that the simplified procedure used here is satisfied.

Finally, the time-lag graphical method is illustrated in Figure 2 for an epoxy resin membrane ($\delta = 6 \times 10^{-2}$ cm). Extrapolation of the linear part of the figure gives: $\theta \approx 26$ h.

Hence:

$$D = \frac{\delta^2}{6\theta} = \frac{(6 \times 10^{-2})^2}{6 \times 26 \times 3600} = 6.4 \times 10^{-9} \text{ cm}^2 \text{ s}^{-1}$$

Similarly, application of the more elaborated theory outlined here (see Equation 14) gives $D \approx 5.9 \times 10^{-9} \text{ cm}^2 \text{ s}^{-1}$. Taking the average value for the diffusion coefficient obtained by the two methods, namely, $D \approx 6.1 \times 10^{-9} \text{ cm}^2 \text{ s}^{-1}$, the solubility of the material can be calculated from the simple relationship: $k = sD$. Hence, $s = k/D \approx 5$, where as calculated above (Table 1), $k \approx 3.5 \times 10^{-8} \text{ cm}^2 \text{ s}^{-1}$. As will be shown elsewhere, the solubility of the material can be obtained more directly from the intercept of the linear part of the figure with the y-axis of the graph (i.e., 'normalized' ^{222}Rn concentration in V_2).

EXPERIMENTAL DIFFICULTIES

Although conceptually very simple, the measurement of k and D is complicated by a number of factors the experimenter should be aware of. Experimental difficulties encountered can be divided broadly into the following categories:

1. Radioactivity measurements;
2. Membrane manufacture;
3. Measurement of some characteristics of membranes;

4. Verification of the 'physical' integrity of the membrane.

Items 1 to 4 will be discussed briefly below.

For low permeability materials, the α -particle count measured by the detector, i.e., [^{222}Rn] in V_2 , may be very low, depending on k or D , and not much different from the background of the detector and its associated electronic circuitry. Hence, counting statistics become an important consideration, and the accuracy of the results are usually subject to great uncertainty.

The physical and chemical characteristics of a given material may not only vary with time but with manufacturer and details of the manufacturing process. Hence, materials measured at different times may give different results. This is not unusual for materials that 'age', e.g., their characteristics deteriorate under exposure to the UV-component of light.

The precise measurement of δ (thickness of the material) is important in the calculation of k (see Equation 30). Measurement of δ becomes increasingly difficult as the thickness of the material decreases. Furthermore, lack of thickness uniformity, a common problem, becomes much more pronounced as δ diminishes.

Verification of the physical integrity of materials used in diffusion studies, and the like, is very difficult. The presence of 'pinholes', microfractures and structural defects (invisible to the naked eye) arising in the manufacturing and handling processes can have a great influence in permeability measurements. This problem is frequently overlooked and might explain some 'conflicting' results reported in the literature.

As previously pointed out, another difficulty that complicates permeability experiments is the variability of certain environmental factors during measurements, such as barometric pressure and temperature, as well as the airflow rate (Q) and [^{222}Rn] in the 'source' volume, V_2 (see Equations 18 and 19).

In view of the above discussion, it is not at all surprising that measurements with the same material conducted at different times, or different samples of the same material measured at the same time, can give results ranging from close agreement to varying by a factor of two, or more.

CONCLUSIONS

The data presented in this report suggest that some of the materials investigated here have permeabilities to ^{222}Rn low enough to be suitable as ^{222}Rn barriers in applications of practical interest such as wall-cover materials in the Sudbury Neutrino Observatory (SNO) Project. However, because of severe mechanical constraints not all materials of low permeability to ^{222}Rn are suitable as ^{222}Rn barriers in the SNO Project. Barrier materials for this specific purpose must meet some basic mechanical requirements such as great resistance to mechanical impact and great mechanical flexibility. Hence, only materials of low permeability that do not easily break, crack, rupture, fissure or develop pinholes are truly suitable for use in conjunction with the SNO Project. These requirements rule out virtually all the materials tested except for the epoxy 'membranes' and MIROC. These materials have permeabilities of the order of $\sim 3.0 \times 10^{-8} \text{ cm}^2 \text{ s}^{-1}$. Because of their relevance in the context of the SNO Project, the properties of the materials will be further investigated and reported in a forthcoming report.

ACKNOWLEDGEMENT

The authors are grateful to Dr. J. Archibald (Dept. of Mining Engineering, Queen's University) for allowing one of us (JB) to reproduce the results of permeability studies conducted on MIROC. The above work is part of a collaborative effort between Dr. Archibald and one of us (J. Bigu).

REFERENCES

1. Lundstrom, J.E. and Bearman, R.J., "Inert gas permeation through homopolymer membranes"; J. Polymer Sci., vol. 17, pp. 97-114, 1974.
2. Henis, M.S. and Tripodi, M.K., "The developing technology of gas separating membranes"; Science, vol. 220, pp. 11-17, 1983.
3. Paul, D.R. and DiBenedetto, A.T., "Diffusion in amorphous polymers"; J. of Polymer Sci. Part C, No. 10, pp. 17-44, 1965.
4. van Amerongen, G.J., "Diffusion in elastomers", in Rubber Chemistry and Technology, pp. 1067-1152.
5. Stein, L., "Chemical properties of radon", in Radon and Its Decay Products - Occurrence, Properties, and Health Effects (P.K. Hopke, Ed.), pp. 240-251, American Chemical Society Series 331, Washington, D.C., 1987.
6. Morse, P.M. and Feshbach, H., "Methods of Theoretical Physics, vol. 1 and 2,, McGraw Hill Book Company, New York, 1953.
7. Ayres, F., "Differential Equations", Schaum's Outline Series; McGraw Hill Book Company, New York, 1952.
8. Bekman, I.N., "Experimental studies of radioactive gas diffusion in solids. II. Evaluation of radioactive decay and growth in the penetrance method"; Soviet Radiochemistry, vol. 23, No. 2, pp. 221-227, 1981.
9. Crank, J., "The Mathematics of Diffusion"; Clarendon Press, Oxford, 2nd Edition, 1975.
10. Bigu, J., Report in preparation and unpublished data.
11. Ward III, W.J., Fleischer, R.L. and Mogro-Campero, A., "Barrier techniques for separate measurements of radon isotopes"; Rev. Sci. Instrum. vol. 48, pp: 1140-1441, 1977.
12. Bigu, J., "An automated multisensor apparatus for comparative membrane radon and thoron permeability studies"; Nuclear Instruments and Methods

in Physics Research, vol. A251, pp. 366-373, 1986.

13. Bigu, J., "Theory and application of radon and thoron progeny monitoring under steady-state and non steady-state radiation conditions. Part II: passive sampling"; Division Report MRP/MRL 85-91(J), CANMET, Energy, Mines and Resources Canada, 1985.
14. Bigu, J., "Theory of diffusion of radon and thoron through membranes under steady-state and time-dependent radiation conditions - parts I and II"; Division Reports MRP/MRL 85-51(TR) Part I, and MRP/MRL 85-52(TR) Part II, CANMET, Energy, Mines and Resources Canada, 1985.
15. Thomas, J.W. and LeClare, P.C., "A study of the two-filter method for radon-222"; Health Phys. vol. 18, pp. 113-122, 1970.
16. Mayya, Y.S. and Kotrappa, P., "Modified double filter method for the measurement of radon or thoron in air"; Ann. Occup. Hyg., vol. 21, pp. 169-176, 1978.

Table 1 - Permeability of several materials to ^{222}Rn

Material	Thickness (δ) (cm)	Permeability (k) (cm^2s^{-1})	Remarks	Manufacturer
Saranex	4.0×10^{-3}	3.7×10^{-8}	-	Dow Canada
Polystyrene	2.6×10^{-2}	1.3×10^{-6}	-	Transilwrap of Canada
Rubber	2.3×10^{-2}	$>1.0 \times 10^{-4}$	Surgical glove	From dental practice
Plastic sheeting	2.3×10^{-2}	1.0×10^{-6}	Transparent pale blue	From Canadian Tire Corp.
Transparency	1.0×10^{-2}	4.0×10^{-7}	-	Xerox
Transalloy	2.6×10^{-2}	1.5×10^{-6}	-	Transilwrap of Canada
Teflon	6.1×10^{-3}	3.5×10^{-7}	-	DuPont
"Anti-thoron" membrane	5.6×10^{-3}	7.9×10^{-8}	-	From Terradex
Rubber	2.5×10^{-2}	1.5×10^{-5}	-	Chase-Walton Elastomers Ltd.
Polyester	5.9×10^{-3}	2.3×10^{-7}	White	3M
Polyester	5.3×10^{-3}	5.3×10^{-8}	Coated	3M
"Yellow membrane"	8.8×10^{-3}	2.1×10^{-7}	Yellow	From Terradex
Polyamide	7.0×10^{-4}	9.5×10^{-10}	Kapton	?
Saran Wrap ⁺	1.3×10^{-3}	1.1×10^{-8}	From Supermarket	?
Gelman Zefluor	1.1×10^{-2}	$>1.0 \times 10^{-4}$	-	Gelman Sciences Inc.
Aluminized mylar	1.0×10^{-3}	5.2×10^{-8}	-	From α -NUCLEAR
Glad Wrap ⁺⁺	1.4×10^{-3}	1.7×10^{-7}	From Supermarket	?
Glad freezer bags	3.5×10^{-3}	7.8×10^{-8}	" "	?
Mylar	9.0×10^{-4}	1.6×10^{-8}	-	DuPont
Al-foil	2.1×10^{-3}	4.6×10^{-8}	From Supermarket	From Stuart House
MIROC I	7.9×10^{-2}	3.1×10^{-8}	Non-uniform thickness	URYLON Canada
MIROC II	11.4×10^{-2}	3.7×10^{-8}	"	" "
MIROC III	16.5×10^{-2}	4.3×10^{-8}	"	" "
EPOXY I	2.5×10^{-2}	3.5×10^{-8}	"	BMS Mfg. Inc.
EPOXY II*	4.9×10^{-2}	1.2×10^{-7}	"	" " "
EPOXY III	5.9×10^{-2}	3.5×10^{-8}	"	" " "
EPOXY IV ⁺	2.7×10^{-2}	4.5×10^{-6}	"	" " "

*Pinholes suspected; ⁺ High density polyethylene; ⁺⁺ Low density polyethylene.

Table 2 - Diffusion length of ^{222}Rn in several materials

Material	Diffusion Length (DL) (cm)	Thickness (δ) (cm)	DL/ δ
Saranex	0.13	4.0×10^{-3}	32.50
Polystyrene	0.79	2.6×10^{-2}	30.38
Rubber	>7.00	2.3×10^{-2}	>304.00
Plastic sheeting	0.69	2.3×10^{-2}	30.00
Xerox transparency	0.44	1.0×10^{-2}	44.00
Transalloy	0.84	2.6×10^{-2}	32.31
Teflon	0.41	6.1×10^{-3}	67.21
"Anti-thoron" membrane	0.19	5.6×10^{-3}	33.93
Rubber	2.67	2.5×10^{-2}	106.80
White polyester	0.33	5.9×10^{-3}	55.93
Coated polyester	0.16	5.3×10^{-3}	30.19
"Yellow membrane"	0.32	8.8×10^{-3}	36.36
Polyamide	2.1×10^{-2}	7.0×10^{-4}	30.00
Saran Wrap	0.07	1.3×10^{-3}	53.85
Gelman Zefluor	6.90	1.1×10^{-2}	627.30
Aluminized Mylar	0.16	1.0×10^{-3}	160.00
Glad Wrap	0.28	1.4×10^{-3}	200.00
Glad freezer bags	0.19	3.5×10^{-3}	54.29
Mylar	0.09	9.0×10^{-4}	100.00
Al-Foil	0.15	2.1×10^{-3}	71.43
MIROC I	0.12	7.9×10^{-2}	1.52
MIROC II	0.13	11.4×10^{-2}	1.14
MIROC III	0.14	16.5×10^{-2}	0.85
EPOXY I	0.13	2.5×10^{-2}	5.20
EPOXY II	0.24	4.9×10^{-2}	4.90
EPOXY III	0.13	5.9×10^{-2}	2.20
EPOXY IV	1.46	2.7×10^{-2}	54.10

Notes:

- DL $= \sqrt{k/\lambda}$, where $\lambda(^{222}\text{Rn}) = 2.1 \times 10^{-6} \text{ s}^{-1}$.
- For more information regarding the materials in Table 2 see Table 1.

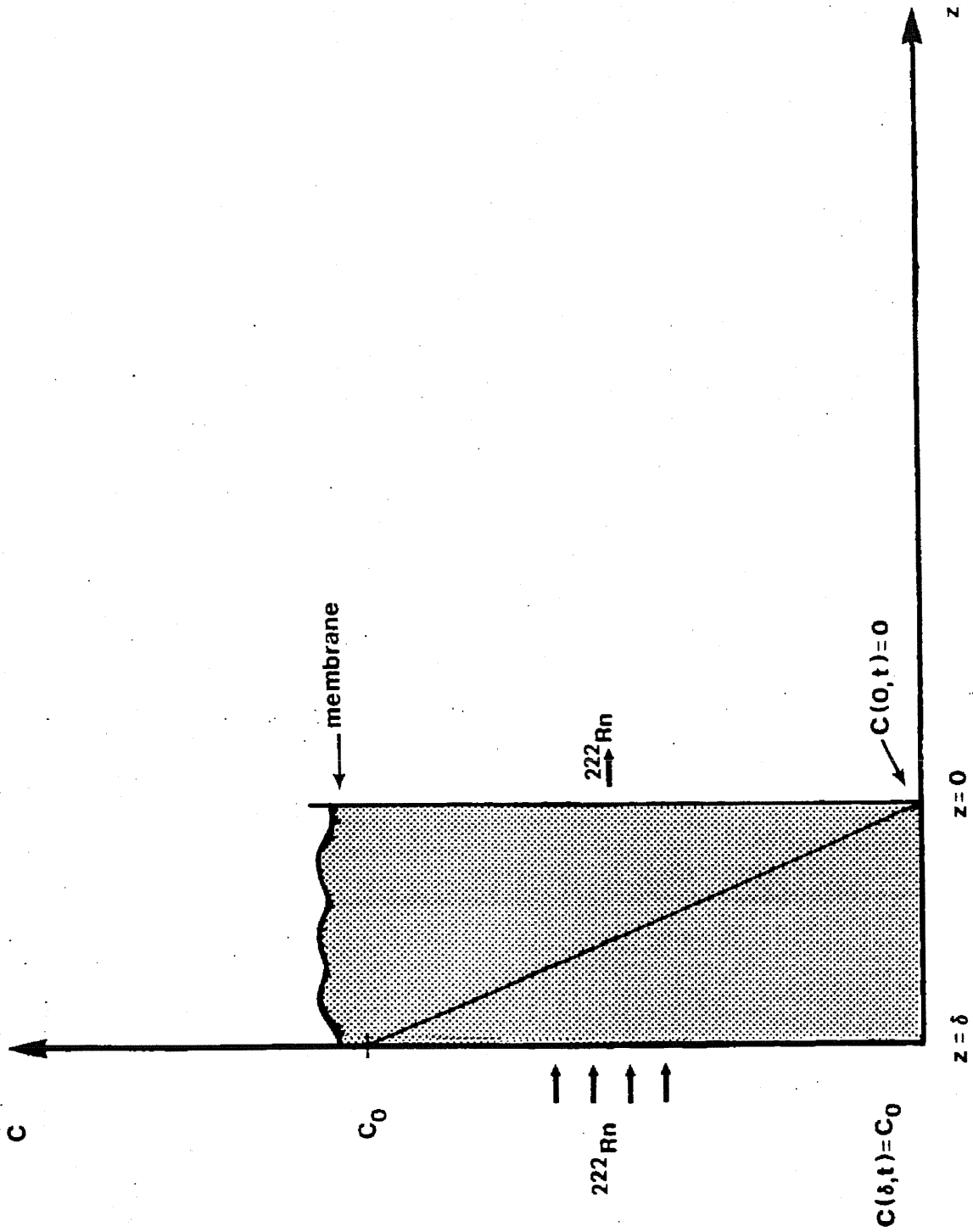


Fig. 1 - Membrane geometry.

TIME-LAG ANALYTICAL PROCEDURE

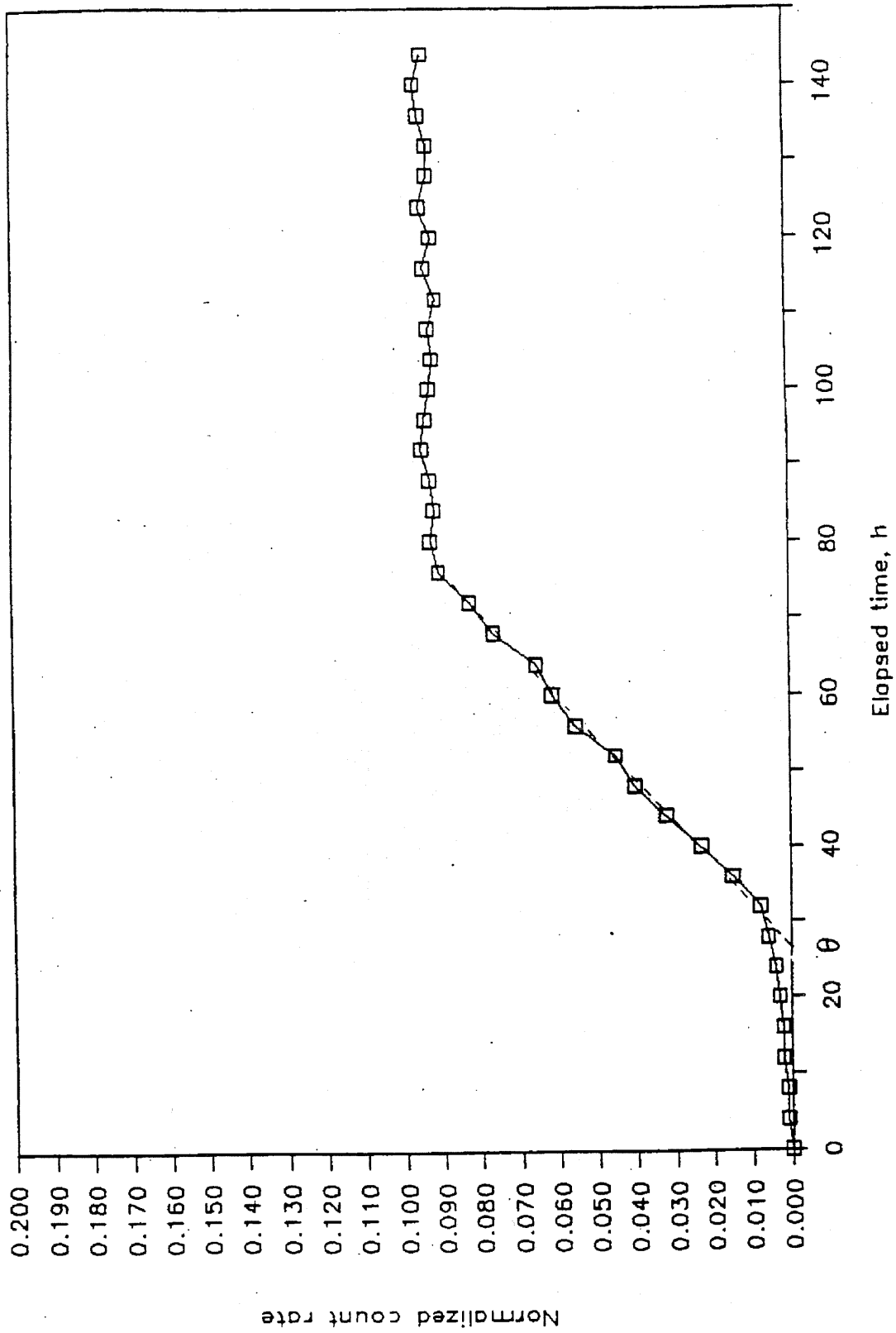


Fig. 2 - Normalized count rate versus elapsed time. Graph used to calculate the time-lag.

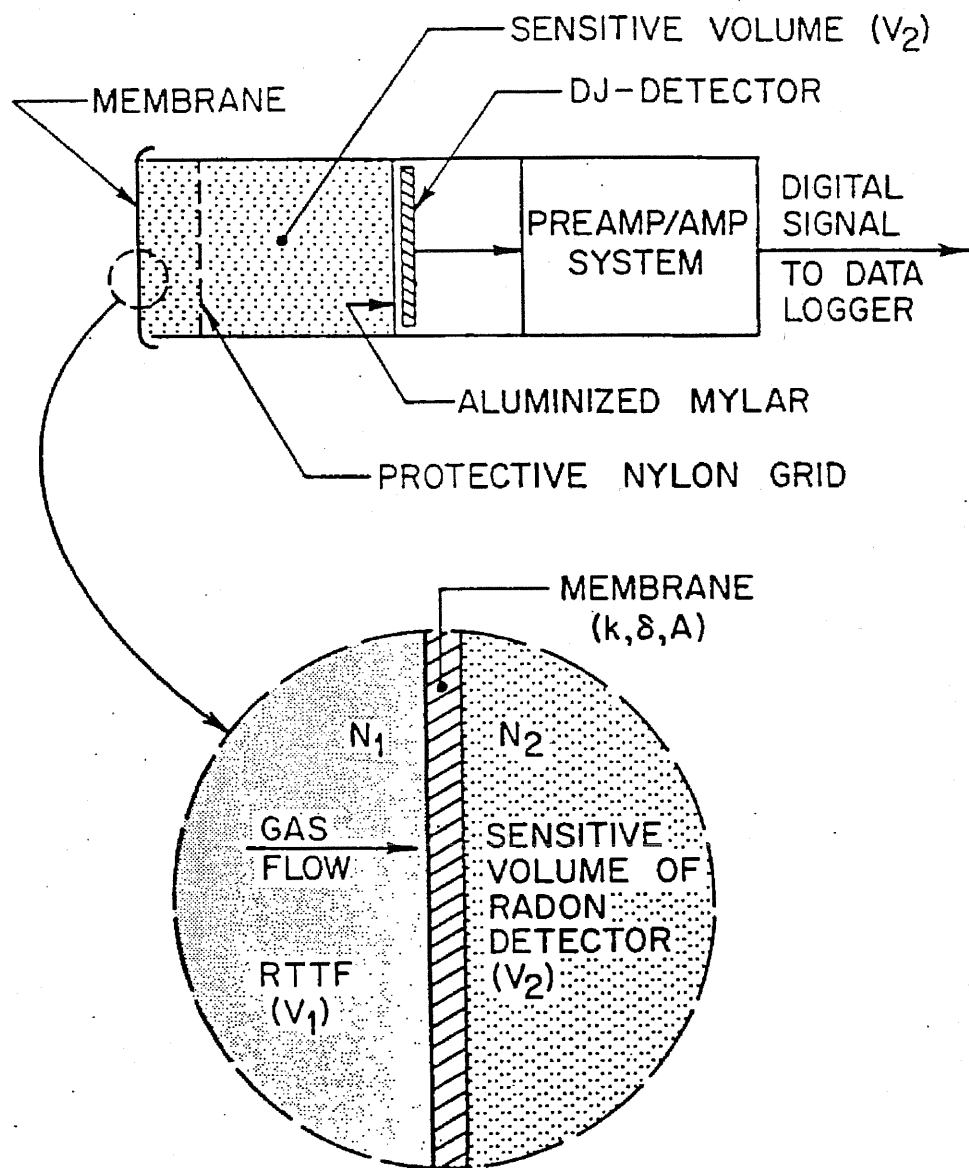


Fig. 3 - Radon-222 monitors showing geometrical arrangement used to determine the permeability of membranes.

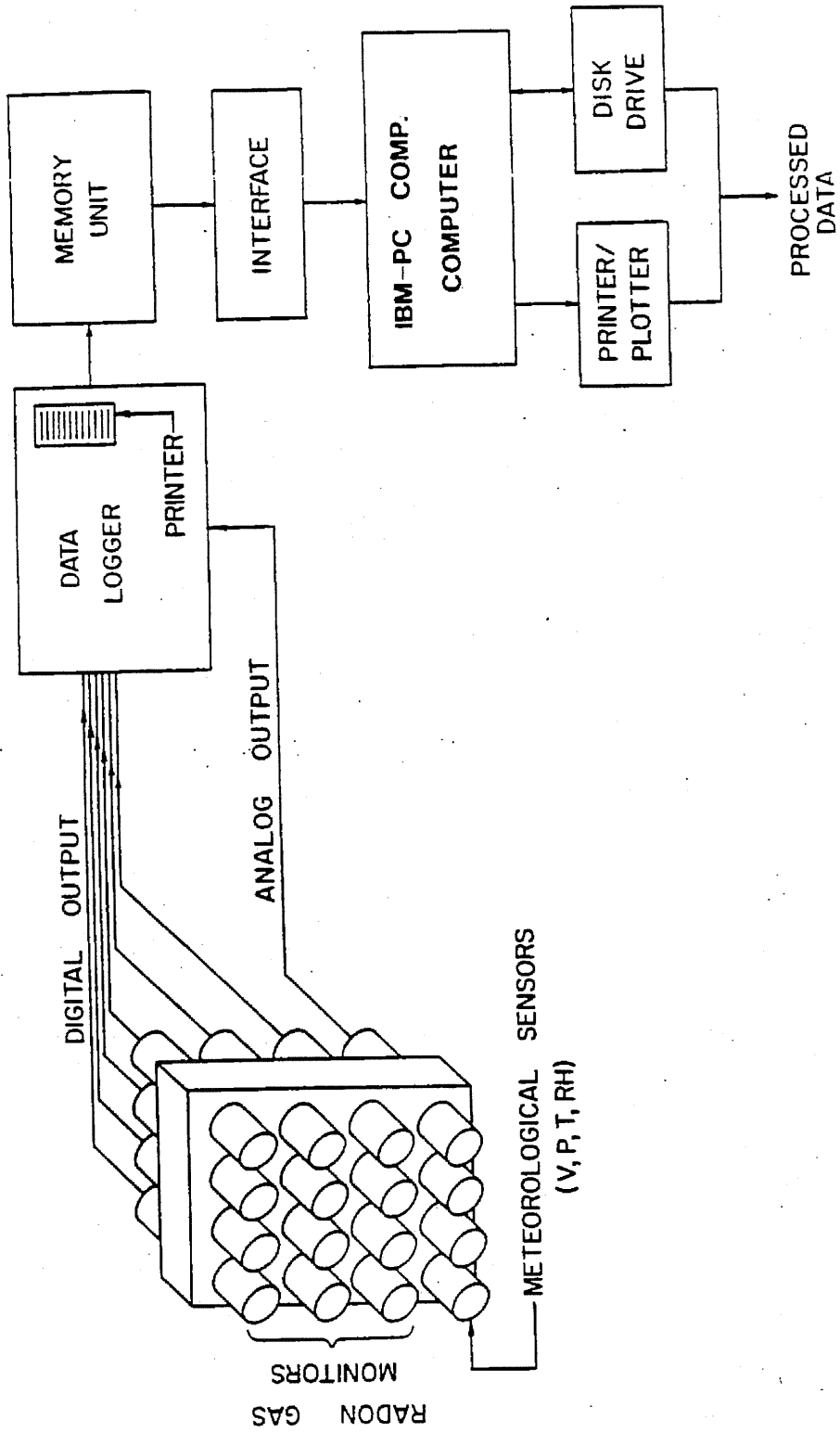


Fig. 4 - 'Multisensor' apparatus used to determine the permeability of membranes.

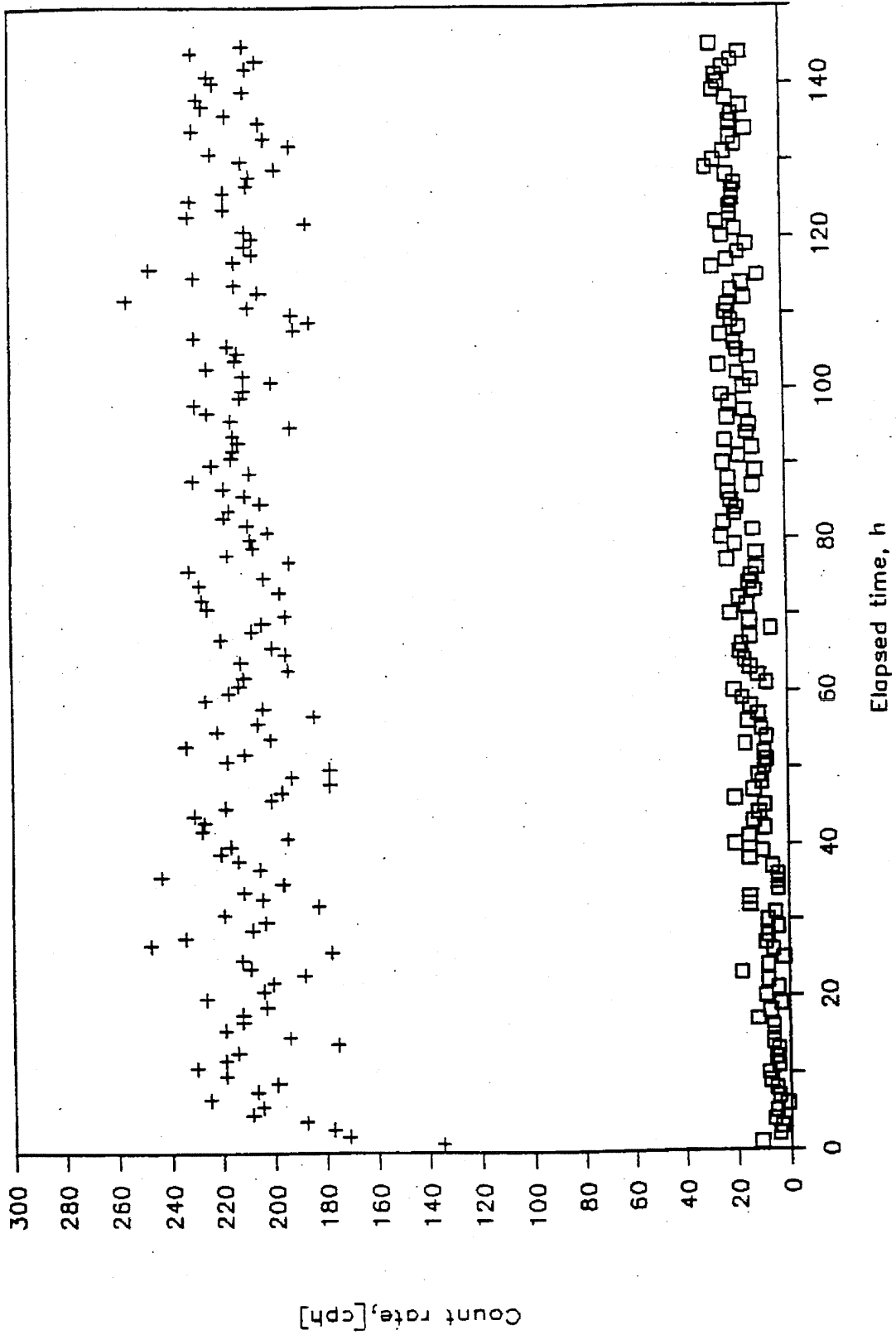


Fig. 5 - Alpha-particle count rate versus elapsed time for a glass fibre filter (upper trace) and a low permeability membrane (epoxy).



Energie, Mines et
Ressources Canada

Energy, Mines and
Resources Canada

CANMET

Centre canadien de la
technologie des
minéraux et de l'énergie

Canada Centre for
Mineral and Energy
Technology

EMANATION AND PERMEABILITY STUDIES AT THE ELLIOT LAKE LABORATORY

J. BIGU AND E.D. HALLMAN

SNO-STR-92-018

The following are data obtained during the months of February and March, 1992.

²²²Rn EMANATION STUDIES

Material	Emanation Rate	
	atoms kg ⁻¹ h ⁻¹	atoms m ⁻² h ⁻¹
Norite	5.03 ± 0.79	248 ± 39*
Shotcrete	52.04 ± 5.35	1968 ± 202*
Boron composite	5.71 ± 0.85	216 ± 32*
Miradri	—	111 ± 2.9
Polyurethane	—	?

+ Only rough estimates (atoms m⁻²h⁻¹) because surface area has not been calculated accurately. Samples still in emanation chambers.

* There have been difficulties in the measurement of this sample because of what seems to be considerable outgassing. It will take another 2-3 weeks, before attempting for the third time.

NOTE: The above values require further verification because calibration factors have to be rechecked, and because changes have been introduced in the emanation chambers and emanation systems.

PERMEABILITY STUDIES

Material	PERMEABILITY k, cm ² s ⁻¹	"STOPPING POWER" R	REMARKS
MIRADRAIN ²	2.28 x 10 ⁻⁸	0.146	1 layer
MIRADRI ¹	1.08 x 10 ⁻⁷	0.057	composite
MIRADRAIN ³	5.41 x 10 ⁻⁸	0.170	2 layers
MIRADRI + MIRADRAIN ⁴	1.20 x 10 ⁻⁷	0.059	1 layer Miradrain + Miradri composite

- 1) Miradri made-up of tar compound sandwiched by polyethylene sheet and paper backing
- 2) Plastic backing material
- 3) "whole" material without Miradri
- 4) "whole" composite

*R is the ratio of the ²²²Rn concentrations measured in the sensitive volume of the detectors for the material under investigation relative to the reference material, i.e. GF filter material. Because k is proportional to the thickness and solubility of the material, it is difficult to compare the properties of materials as ²²²Rn barriers unless all the materials investigated have the same, say, thickness. For this reason, and particularly for Miradri, the R values are given. This topic will be discussed shortly.

Note The increase of k with the increasing thickness of the material is more apparent than real. This is so because $k \propto \delta$ (thickness) and often an additional increase in δ does not bring about any significant improvement in R. (See SNO-STR-91-069)

ULTRAHIGH WATER PURIFICATION SYSTEM

A ultrahigh water purification system has been built which is now operational. Some preliminary tests are now being conducted to ensure that the system produces water of the desired purity. The system has been designed to carry out ²²²Rn emanation studies of different materials in water.


 Énergie, Mines et
Ressources Canada

 Energy, Mines and
Resources Canada

CANMET

 Centre canadien de la
technologie des
minéraux et de l'énergie

 Canada Centre for
Mineral and Energy
Technology

SNO-STR-92-037

²²²Rn EMANATION FROM MATERIALS

J. BIGU AND D. HALLMAN.

Emanation of ²²²Rn from three materials has been measured recently in the laboratory. Radon-222 flux density measurements have been conducted at level 6800 in the Creighton mine (Inco, Sudbury) in an area where a layer of shotcrete had been applied to the rock (Norite) wall face. In addition, measurements of the concentrations of ²²²Rn, ²²⁰Rn, and their short-lived decay products, were also carried out at the above underground location.

Radon-222, ²²⁰Rn and their progeny were determined by the two-filter method. Flux density measurements were carried out by two methods, namely, the accumulator (closed-loop, continuous monitoring) method, and the "open-loop" method. In the first case, ²²²Rn concentration was determined using a scintillation cell in a continuous fashion. In the second case, the ²²²Rn concentration was measured by means of electrets. The results of the measurements described above are given below:

²²²Rn, ²²⁰Rn, and Progeny Concentration

$$\text{PAEC (Rn)} = 0.223 \pm 0.020 \mu\text{Jm}^{-3}$$

$$\text{PAEC (Tn)} = 0.117 \pm 0.008 \mu\text{Jm}^{-3}$$

$$\text{PAEC(Tn)/PAEC(Rn)} = 0.52$$

$$[^{222}\text{Rn}] = 99.2 \pm 22.4 \text{ Bqm}^{-3}$$

$$[^{220}\text{Rn}] = 237.7 \pm 54.8 \text{ Bqm}^{-3}$$

$$T = 29.6 - 30^\circ\text{C}$$

$$\text{RH} = 64.4 - 67\%$$

$$P \sim 115 \text{ kPa}$$


 Énergie, Mines et
Ressources Canada

 Energy, Mines and
Resources Canada

CANMET

 Centre canadien de la
technologie des
minéraux et de l'énergie

 Canada Centre for
Mineral and Energy
Technology

EMANATION STUDIES IN THE LABORATORY

Material	Emanation Rate	Surface Area
Polyurethane (201-15FR)	3.9 ± 1.7 atom $m^{-2}h^{-1}$	2.49 m^2
MIRADRAIN (GRAY)	2.4 ± 2.3	1.00 m^2
GEOTEXTILE	0.1 ± 1.0	1.50 m^2

* In all the cases shown above, the surface area has been counted only once, per sheet, even for the case of the MIRADRAIN sample which was made up of one layer of extruded material glued together to a smooth layer of the same material. It should be noted that the geotextile material was removed from the MIRADRAIN. Furthermore, the surface area of the extruded layer is much larger than the area corresponding to the smooth layer. The surface area of the latter has been taken, and given in the above table.

FLUX DENSITY MEASUREMENTS

The values obtained for the ^{222}Rn flux density were as follows:

Accumulator method (continuous monitoring)

$$\begin{aligned}
 J(Rn) &= 7.92 \times 10^2 \text{ atoms } m^{-2}s^{-1} \\
 &= 1.67 \times 10^{-3} \text{ Bq } m^{-2}s^{-1} \\
 &= 4.50 \times 10^{-2} \text{ pCi } m^{-2}s^{-1}
 \end{aligned}$$

Open-Loop/electret method

$$\begin{aligned}
 J(Rn) &= 2.1 \times 10^3 \text{ atoms } m^{-2}s^{-1} \\
 &= 4.4 \times 10^{-3} \text{ Bq } m^{-2}s^{-1} \\
 &= 0.12 \text{ pCi } m^{-2}s^{-1}
 \end{aligned}$$

NOTES:

The two methods differ by a factor of about 2.7. Measurements are subject to large uncertainties because of the roughness of the wall surface, which makes sealing of the containers to the wall very difficult. We cannot ensure that measurements were conducted under leakfree conditions.

SUDBURY NEUTRINO OBSERVATORY
RADON MEASUREMENTS - JANUARY 1992
6800 ft LEVEL - CREIGHTON MINE

E.D. Hallman, D.L. Cluff, and D. Cloutier
Laurentian University
SNO-STR-92-005
February 3, 1992

INTRODUCTION:

To establish the acceptability of the proposed liner design for the SNO detector cavity, levels of radon present in the compressed air supply at the 6800 ft level of the Creighton Mine, and radon emanation measurements from typical rock surfaces coated with shotcrete, must be evaluated. This report gives results from the first set of measurements in the evaluation program. Two sets of results for radon and radon decay products in the compressed air, and in the mine air are reported. Also measured was the radon emanation from the rock surfaces of a closed 2 inch drill hole.

THE RADON MEASUREMENTS:

Radon measurements were made for the compressed air supply from an outlet at the 'old' wash station - a widened section of the entrance drift for the SNO laboratory (location A). Mine air measurements were also made at this location as well as at the junction of the control and utility rooms (location B). The drill hole for the radon emanation measurement was the lower of two blind holes on the north side of the old wash station, used in a previous emanation study (SNO-STR 90-129).

A portable radon monitor (Pylon Model R2000) was used with 180 mL scintillation cells (for radon measurements) or a 30 mm diameter scintillator tray (for radon decay product counts from 25 mm 0.8 μ m air filters. Radon levels (pCi/L) and decay product levels (in Working Level units WL) are listed in Tables 1 and 2. Decay product activities were found using the Kusnetz method. In all cases, air filtering was carried out for 10 minutes at an air flow rate of approximately 13 L/min.

To sample the compressed air lines, a 4 L flow-through sampling canister was set up as shown in Figure 1. Air flow rates and purging times are listed in Table 1.

Figure 1: Compressed air sampling system

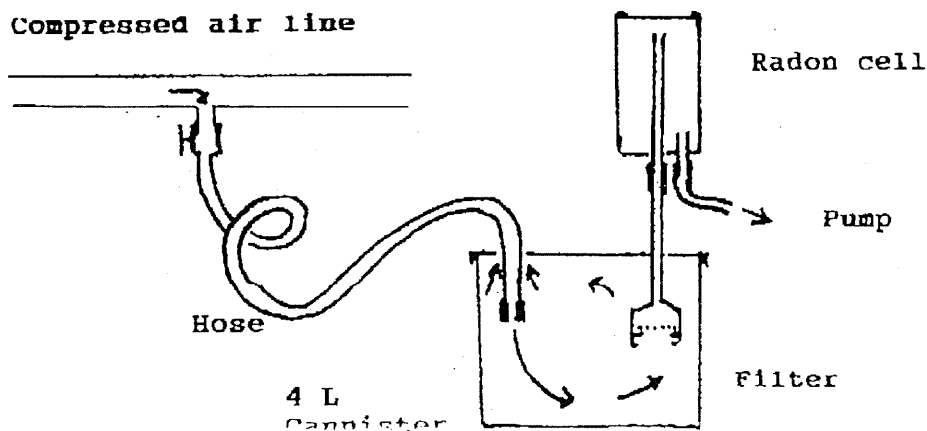


Table 1: Compressed Air Radon and Radon Decay Products

Cell # (filter #)	Background (opm)	Net Counts (opm)	R(Rn)* (pCi/L)	Air Filter Vol.(L) (opm)	W.L.	F
4 (3)	0.50	3.00	3.51 (0.5)	129 0.85	0.0001	0.003
1 (1)	1.15	0.86	1.5 (0.8)	130 1.75	0.0008	0.04

* average of two determinations corrected for decay of the radon sample

The cell # 4 compressed air sample was collected at an air flow rate of 100 L/min, following a 2 minute purge.

The cell # 1 compressed air sample was collected at an air flow rate of 1000 L/min, following a 35 minute purge.

From Table 1, it is evident that radon concentrations of 2.5 +/- 1.0 pCi/L are typical of the compressed air on the 6800 ft level. There is a suggestion that the longer purge time and higher flow rate for the second sample results in lower radon levels. A conservative upper limit for radon content would appear to be 4 pCi/L - a value typical of the mine air which enters the compressed air system at the underground compressor station. Very little radon decay products are observed in this air (average F = 0.02 +/- 0.02), compared to typical mine air. This result is understandable, given the large interior surfaces of the supply pipes which probably serve as scavengers of the decay products.

Table 2: Mine drift air Radon and Radon Decay Products

Cell # (filter #)	Background (opm)	Net Counts (opm)	R(Rn)* (pCi/L)	Air Filter Vol.(L) (opm)	W.L.	F
2 (2)	1.15	0.83	1.3 (0.8)	130 29	0.0058	0.45
5 (5)	0.73	2.23	3.0 (0.3)	130 16.3	0.0033	0.11

* average of two determinations corrected for decay of the radon sample

The cell # 2 sample was collected at location A

The cell # 5 sample was collected at location B

Note: 1 W.L. is the activity of decay products when 100 pCi/L ²²²Rn is in equilibrium with its decay products.

F = 100 x W.L./R(Rn) is an equilibrium factor, indicating the degree of decay product loss through ventilation or plate-out.

The radon results of Table 2 indicate an average radon level of 2.2 +/- 0.8 pCi/L in the mine air. Radon decay product levels averaged 0.0046 +/- 0.0015 W.L., with an average F = 0.28. These results compare quite well with earlier measurements made in June 1990 (SNO report SNO-STR -90-129), where radon levels of 3.3 +/- 0.8 pCi/L and decay product levels of 0.0058 +/- 0.0016 were found. The lower values of the latest measurements would be consistent with the better ventilation now in effect at the sample locations.

Drill Hole Radon Measurements

Radon scintillation cell # 3 (volume = 180 mL) was evacuated, and connected to an opening into the blind drill hole at the wash station which had been plugged for many months. The radon activity of the air sample obtained was measured at two times, and results were corrected for radon decay. The average radon activity was found to be 15.3 +/- 1.5 pCi/L (with a cell count rate of 9.81 cpm). This compares very well with the measurements of July 1990 for the same hole, where a count rate of 13.0 x 0.73 (correction for cell volume difference) = 9.45 cpm was observed.

Reference:

E.D. Hallman and D.L. Cluff, Radon and Dust Measurements - July 1990
Sudbury Neutrino Observatory Site Report SNO-STR-90-129(1990).

From HALLMAN@NICKEL.LAURENTIAN.CA Thu Sep 10 18:01 EDT 1992
 Received: from nickel.laurentian.ca by mips2.Phy.QueensU.CA (5.61/4.7)
 id AA10685; Thu, 10 Sep 92 18:01:19 -0400
 Received: from NICKEL.LAURENTIAN.CA by NICKEL.LAURENTIAN.CA (PMDF #12037) id
 01GOMN2XHZSG8WW39A@NICKEL.LAURENTIAN.CA>; Thu, 10 Sep 1992 18:07 EST
 Date: Thu, 10 Sep 1992 18:07 EST
 From: HALLMAN@NICKEL.LAURENTIAN.CA
 Subject: Shotcrete Rn emanation update - Doug
 To: bar@mips2.phy.queensu.ca
 Message-Id: <01GOMN2XHZSG8WW39A@NICKEL.LAURENTIAN.CA>
 X-Vms-To: IN*"bar@mips2.phy.queensu.ca"
 X-Vms-Cc: HALLMAN
 Status: R

SNO-STR-92-064

Sudbury Neutrino Observatory

Underground Radon Measurements at the Creighton Mine:

I - Radon Emanation from Shotcrete

J. Bigu* and E.D. Hallman
 Laurentian University SNO Group

September 10, 1992

Radon (²²²Rn) emanations from the rock and sprayed concrete surfaces near the SNO cavity on the 6800 ft level of the Creighton Mine, have been measured by several techniques. This report summarizes measurements made using monitoring equipment from the Elliot Lake Laboratory (CANMET), with two techniques: A - accumulator method, in which the build-up of radon in a sealed canister is monitored continuously as the emanation and subsequent radon decay occurs, and B - open-loop/electret method in which radon additions to the air flowing through the canister is monitored by means of two electret detectors. Initial measurements were made on a natural ("popcorn" finish) shotcrete surface, at the approximate mid-point of the west wall of the control room drift (Location 1). The rough, uneven nature of the surface made the sealing of the canisters to the wall difficult and some small air leaks may have been present. A second set of measurements were made on a flat specially-prepared ("trowelled and broomed") shotcrete surface approximately 20 feet from the entrance of the personnel drift, about 5 ft from the drift floor on the west wall (Location 2). In both locations, a shotcrete layer of from 4 - 6 inches thick had been sprayed on the norite rock of the drift and no voids were evident. Results were analyzed using standard techniques to give radon emanations as listed in Table 1.

Table 1: Radon Flux Density from Shotcrete/Rock Wall Surfaces

Date	Location	Radon Flux Density J(Rn)	Technique
April 1992	1	7.92 x 10 ² atoms.m ⁻² .s ⁻¹ 1.67 x 10 ⁻³ Bq.m ⁻² .s ⁻¹ 4.50 x 10 ⁻² pCi.m ⁻² .s ⁻¹	A
July 1992	1	2.1 x 10 ³ atoms.m ⁻² .s ⁻¹	B
August 27, 1992	2	5.29 x 10 ³ atoms.m ⁻² .s ⁻¹	A and B**

** For these measurements, results using both techniques were identical to

in location 1 is felt to be related to the difficulty in sealing the canisters to the surface at this location.

Since the radon emanating from the shotcrete surfaces has diffused from uranium/radium sites in the shotcrete or underlying rock, measurements of uranium concentrations in these materials were made, so that diffusion lengths for radon in the wall surfaces could be estimated. Table 2 lists uranium (U238) and thorium (Th232) concentrations in the shotcrete mix used at location 2, and for norite rock (averaged) in this vicinity. Assuming a value of the radon flux density of 5000 atoms.m⁻².s⁻¹, and using a value of 2.0 ug/g for the U238 concentration (assumed in equilibrium with its decay products), a diffusion depth of order 10 cm can be estimated for this geometry. Approximately 60,000 decays of the uranium (and of each of the decay products) occur per m³ per s.

Table 2: Concentrations of U and Th in wall materials at the monitoring sites

Material	Location	Concentrations	
		U	Th (ug/g)
shotcrete (dry mix)	2	2.60 +/- .36	6.11 +/- .17
norite	SNO cavity (4 sample average)	1.15 +/- .3	5.50 +/- .5

A report summarizing all radon in mine air and surface emanation measurements made to date at the SNO sites in the Creighton Mine is in preparation.

* Research Scientist, Elliot Lake Laboratories, CANMET